Published in final edited form as:
Dev Cell. 2013 February 25; 24(4): 359–371. doi:10.1016/j.devcel.2013.01.009.

PERIPHERAL NERVE-DERIVED CXCL12 AND VEGF-A REGULATE THE PATTERNING OF ARTERIAL VESSEL BRANCHING IN DEVELOPING LIMB SKIN

Wenling Li[*], **Hiroshi Kohara**[§], **Yutaka Uchida**[*], **Jennifer M. James**[*], **Kosha Soneji**[*], **Darran G. Cronshaw**[#], **Yong-Rui Zou**[#], **Takashi Nagasawa**[§], and **Yoh-suke Mukouyama**[*,†]

[*]Laboratory of Stem Cell and Neuro-Vascular Biology Genetics and Developmental Biology Center National Heart, Lung, and Blood Institute National Institutes of Health Building 10/6C103, 10 Center Drive, Bethesda, MD20892

[§]Department of Immunobiology and Hematology Institute for Frontier Medical Sciences, Kyoto University 53 Kawahara-cho, Shogoin, Sakyo-ku, Kyoto 606-8507, Japan

[#]Division of Hematology, Center for Biologics Evaluation and Research, Center for Autoimmune and Musculoskeletal Diseases, Feinstein Institute for Medical Research 350 Community Drive Manhasset, NY 11030

SUMMARY

In developing limb skin, peripheral nerves provide a spatial template that controls the branching pattern and differentiation of arteries. Our previous studies indicate that nerve-derived VEGF-A is required for arterial differentiation but not for nerve-vessel alignment. In this study, we demonstrate that nerve-vessel alignment depends on the activity of Cxcl12-Cxcr4 chemokine signaling. Genetic inactivation of Cxcl12-Cxcr4 signaling perturbs nerve-vessel alignment, and abolishes arteriogenesis. Further *in vitro* assays allow us to uncouple nerve-vessel alignment and arteriogenesis, revealing that nerve-derived Cxcl12 stimulates endothelial cell migration, while nerve-derived VEGF-A is responsible for arterial differentiation. These findings suggest a coordinated sequential action in which nerve-Cxcl12 functions over a distance to recruit vessels to align with nerves and subsequent arterial differentiation presumably requires a local-action of nerve-VEGF-A in the nerve-associated vessels.

INTRODUCTION

The vascular system, which is a vast network of arteries, veins and capillaries, is crucial for organ development during embryogenesis, as well as for organ maintenance and reproductive function in the adult. Despite the significance of the vascular system, the process by which it adopts a particular blood vessel branching pattern is poorly understood. The patterning is thought to occur by remodeling a pre-existing primary capillary network into a highly branched hierarchical vascular tree. It has been suggested that environmental factors may function as guidance cues to form a tissue-specific vascular pattern. The loss of guidance cues has been shown to lead to abnormal vascularization, which contributes to a number of pathologically identifiable conditions (reviewed in Dorrell and Friedlander,

[†] Author for correspondence: Tel: (301) 451 1663 FAX: (301) 480 1581 mukoyamay@mail.nih.gov.

2006). Although guidance molecules capable of inducing endothelial cell sprouting have been identified (reviewed in Adams and Eichmann, 2010), the source tissue or cells for these guidance molecules, however, is less clear. In addition, the role of non-vascular tissues in patterning the emerging vascular network remains largely unknown.

To study the elaborate and intricate processes of vascular branching, a directly observable vascular network with an anatomically recognizable pattern is an ideal model. Thus, we developed a model system using the embryonic limb skin vasculature. The embryonic limb skin has a highly stereotypic and recognizable vascular branching (Mukouyama et al., 2002). During angiogenesis in the embryonic limb skin, the arterial branching pattern coincides with the branching pattern of pre-established sensory nerves. At E13.5, there is no association between sensory nerves and blood vessels and no detectable arterial marker expression in the capillary plexus. By E14.5, vascular remodeling occurs and these remodeled vessels associate with sensory nerves. At this stage, some nerve-associated vessels express arterial markers such as ephrinB2 and neuropilin 1 (Nrp1), but the other nerve-associated smaller-diameter vessels do not yet express them. By E15.5, most nerve-associated vessels express arterial markers. The extensive time-course analysis reveals that arterial differentiation is immediately preceded by nerve-vessel alignment (Mukouyama et al., 2002). In *Ngn1*$^{-/-}$*; Ngn2*$^{-/-}$ double homozygous mutant embryos lacking peripheral axons and Schwann cells in the embryonic skin, the primitive capillary plexus forms normally but proper arterial differentiation fails to occur. Moreover, in *Sema3A*$^{-/-}$ mutants where the pattern of sensory nerve branching is disrupted, the arterial branching pattern still follows the trajectory of the disorganized nerves (Mukouyama et al., 2002). These genetic studies in mouse embryos suggest that arterial differentiation is dependent on the presence of nerves and nerves provide a template that instructively patterns the branching of the emerging arterial vascular network.

What signals control nerve-vessel alignment and arterial differentiation? Genetic studies in mouse and zebrafish embryos demonstrated that activation of VEGF-A and Notch signaling pathways is required for arterial differentiation (Lawson et al., 2002; Mukouyama et al., 2002; Visconti et al., 2002). Inactivation of nerve-derived *Vegf-a* or endothelial neuropilin 1 (*Nrp1*), a co-receptor for VEGF-A, indeed led to defects in arterial differentiation of limb skin vasculature (Mukouyama et al., 2005). However, nerve-vessel alignment was unaffected in these conditional mutants (Mukouyama et al., 2005). This observation suggests that unidentified nerve-derived signals might govern the nerve-vessel alignment in the limb skin. It is therefore probable that two distinct mechanisms exist to control nerve-mediated arterial branching patterns: one controlling arterial differentiation, and another for vessel branching and alignment with nerves.

Like VEGF signaling, tyrosine kinase receptor signaling systems have been implicated in vascular development (reviewed in Coultas et al., 2005; Risau, 1997). *Loss-of-function* mutations in many of the genes encoding these receptors result in embryonic lethality due to defects in early vascular development (reviewed in Argraves and Drake, 2005). This leaves open the possible contribution of other ligand-receptor signaling pathways for vascular branching. Of the potential candidate signals, we considered the G-protein coupled receptor (GPCR) signaling pathway, which has diverse functions in vascular development such as endothelial cell proliferation, migration and cell death in a tissue specific manner. Among the GPCRs, it has been demonstrated that activation of the CXC motif chemokine receptor Cxcr4 by its soluble ligand Cxcl12 (also known as SDF1) influences endothelial sprouting in the developing gut (Tachibana et al., 1998; Ara et al., 2005), kidney (Takabatake et al., 2009) and retina vasculature (Strasser et al., 2010). In zebrafish embryos, endoderm-derived Cxcl12 is essential for complete connection of the developing Cxcr4^{+} lateral dorsal aorta, the major arterial vessel in the anterior vasculature (Siekmann et al., 2009). Cxcl12 also

directs trunk lymphatic network formation, resulting in a co-alignment of lymphatic and blood vessels (Cha et al., 2012). These observations suggest that Cxcl12-Cxcr4 signaling may contribute to angiogenic sprouting from the larger artery and to the linking of adjacent endothelial cells by guiding filopodium extension. However, the possible contribution of Cxcl12-Cxcr4 signaling to the formation of vascular branching patterns via remodeling of a pre-existing capillary network has not been explored.

In this study, we demonstrate genetic evidence in mice that Cxcl12-Cxcr4 signaling plays an essential role in nerve-mediated arterial branching resulting in nerve-artery alignment in the limb skin. Peripheral nerves express Cxcl12, whereas its receptor Cxcr4 is expressed by a subset of endothelial cells in the capillary network before remodeling. After remodeling, the Cxcr4 expression is restricted to larger nerve-associated arteries. Our *in vitro* experiments suggest that Cxcl12-Cxcr4 signaling is a major determinant for nerve-mediated endothelial cell migration but not arterial differentiation. In mutants lacking *Cxcl12, Cxcr4* or endothelial *Cxcr4*, arteries in the limb skin fail to properly align with nerves. Taken together with our previous genetic finding that lack of Schwann cells prevents proper vascular remodeling and nerve-vessel alignment (Mukouyama et al., 2002), these data suggest that Cxcl12 is a nerve-derived vascular patterning signal controlling proper nerve-artery network formation through endothelial Cxcr4 in the developing limb skin.

RESULTS

Expression of Cxcl12 and Cxcr4 in the developing limb skin

We first characterized the expression of 24 chemokine ligands in dorsal root sensory ganglia (DRG) and 17 receptors in PECAM 1^+ limb skin endothelial cells isolated by fluorescence-activated cell sorting (FACS), using a RT-PCR array method (data not shown). Among those tested, a semi-quantitative RT-PCR analysis confirmed the expression of Cxcl12, and its receptors Cxcr4 and Cxcr7 at embryonic day (E) 13.5 and 15.5, the stages at which vascular remodeling occurs, resulting in nerve-vessel alignment (Supplemental Figures S1A and S1B). Whole-mount immunohistochemical staining was then used to examine the distribution of these proteins in the limb skin from E13.5 through E15.5. To detect Cxcl12 expression, we used *Cxcl12*^{GFP} knock-in embryos expressing GFP from the *Cxcl12* locus (Ara et al., 2005). At E13.5, the expression of Cxcl12 was apparent in all the nerves in the limb skin, especially in nerve-associated migrating Schwann cells, which are identified by the glial marker Brain Fatty Acid Binding Protein (BFABP) (Figures 1A and 1C, Supplemental Figures S1E and S1F, open arrows; Kurtz et al., 1994). The expression persisted at E15.5, after nerve-blood vessel alignment had occurred (Figures 1B and 1D, open arrows). If nerve-derived Cxcl12 plays an instructive role in recruiting arterial vessels to align with nerves, we might expect that a subset of vessels would express higher levels of its receptors before the alignment occurs. In accordance with this prediction, we detected a mosaic distribution of Cxcr4 protein on capillary vessels near the nerves at E13.5 (Figures 1E and 1G, arrowheads). At this stage, there was little difference in the expression of the arterial transcription factors *Hey1* and *Hey2* mRNAs and the venous markers *EphB4, COUPTFII* and *BMX* mRNAs between $Cxcr4^+$ and $Cxcr4^-$ endothelial cells (Supplemental Figures S1C and S1D). By E15.5, however, Cxcr4 expression was restricted only to nerve-associated arteries (Figures 1F and 1H, arrowheads; Supplemental Figures S1G and S1H, arrowheads). Interestingly, Cxcr4 expression was detected in small-diameter arteries that aligned with the disorganized nerves in *Sema3A*$^{-/-}$ mutants, suggesting that the pattern of $Cxcr4^+$ arteries depends on the pattern of nerve branching (Supplemental Figures S1I versus S1J, S1K versus S1L, open arrows and arrowheads). In contrast, Cxcr7 expression appeared to be uniformly distributed in the limb skin without any vessel specific restriction (data not shown). These results suggest that nerve-derived Cxcl12 and endothelial Cxcr4 may be responsible for nerve-vessel alignment in the limb skin.

Failure of nerve-vessel alignment in *Cxcl12* and *Cxcr4* homozygous mutants

To examine the functional role of Cxcl12-Cxcr4 signaling in nerve-vessel alignment, we carried out a genetic analysis of nerve-vessel association in *Cxcl12*$^{-/-}$ and *Cxcr4*$^{-/-}$ mutant embryos. In developing limb skin, peripheral nerves associate with remodeled vessels (Figures 2A and 2G, open arrows and arrowheads). In *Cxcl12*$^{-/-}$ and *Cxcr4*$^{-/-}$ mutants, nerve-vessel alignment was greatly disrupted (Figures 2A versus 2B and 2C, 2G versus 2H and 2I, open arrows and arrowheads), though some vascular remodeling occurred with disorganized branching patterns (Figures 2B, 2C, 2E, 2F, 2H, 2I, 2K and 2L, arrowheads). We quantified the amount of nerve-vessel alignment by measuring the fractional length of nerves associated with vessels. Compared to control littermates, a marked reduction (~60%) of nerve-vessel alignment was observed in *Cxcl12*$^{-/-}$ and *Cxcr4*$^{-/-}$ mutants (Figure 2M), although there was no significant difference in vascular density between these mutants and control littermates (Figure 2N). When tested for innervation, normal innervation accompanied by BFABP^{+} migrating Schwann cells was observed in these mutants (Supplemental Figures S2A versus S2B and S2C, S2D versus S2E and S2F, S2G versus S2H and S2I, arrows). There was no statistically significant difference in the number of BFABP^{+} Schwann cells between control littermates and *Cxcl12*$^{-/-}$ or *Cxcr4*$^{-/-}$ mutants (Supplemental Figure S2J). Indeed, embryos bearing endothelial cell-specific deletion of *Cxcr4* (*Tie2-Cre; Cxcr4*$^{flox/-}$) exhibited similar defects to those observed in conventional *Cxcl12*$^{-/-}$ or *Cxcr4*$^{-/-}$ mutants (Supplemental Figures S2K versus S2L, S2M versus S2N, open arrows and arrowheads; S2O). Of note, the endothelial-specific *Cxcr4* mutants exhibited normal innervation with BFABP^{+} Schwann cells as those observed in control littermates (Supplemental Figures S2P versus S2Q, S2R versus S2S, arrows; S2T). These data suggest that defective nerve-vessel alignment is due to lack of Cxcl12-Cxcr4 signaling in endothelial cells.

To rule out the possibility that the observed failure of nerve-vessel alignment might have been a result of cardiac defects or vascular failure in major vessels, we examined gross morphology of the null mutants' heart and trunk vasculature. We did not observe any morphological change in major vessels of the forelimb (Supplemental Figures S3A versus S3B and S3C, arrowheads). Trunk vasculature, heart endocardium and myocardial trabeculation appeared unaffected in the mutants at E15.5 (Supplemental Figures S3D versus S3E and S3F, H&E staining; S3G versus S3H and S3I, S3J versus S3K and S3L, arrowheads; S3M versus S3N and S3O, open arrowheads). Taken together, these data indicate that the observed failure of nerve-vessel alignment in the limb skin is not a consequence or a cause of global vascular or cardiac defects.

Defective arterial differentiation and smooth muscle coverage in *Cxcl12* and *Cxcr4* homozygous mutants

We next examined whether the perturbation in nerve-vessel alignment is accompanied by defective arteriogenesis. To assess this, we analyzed the expression of arterial markers: neuropilin 1 (Nrp1) and connexin 40 (Cx40). In control littermates, nerves associated with small- and middle-diameter branched arterial vessels (Figures 3A, 3D, 3H, 3K, arrowheads). Nrp1 expression was detected both in small- and middle-diameter arteries (Figures 3A and 3D, arrowheads), while Cx40 expression was relatively specific for middle-diameter arteries (Figures 3H and 3K, arrowheads). Nerve-associated vessels were covered by αSMA^{+} smooth muscle cells (Figures 3O and 3R, arrowheads). In *Cxcl12*$^{-/-}$ and *Cxcr4*$^{-/-}$ mutants, the expression of these arterial markers was greatly reduced in small- and middle-diameter branched vessels (Nrp1: Figures 3D versus 3E and 3F, arrowheads, 3G; Cx40: 3K versus 3L and 3M, arrowheads, 3N). Weak expression of Nrp1 was detected in some small-diameter branched vessels located in relatively close proximity to nerves (Figures 3E and 3F, open arrowheads). Cx40 expression was almost undetectable in middle-diameter vessels (Figures

3L and 3M, arrowheads). There was a clear reduction of αSMA$^+$ smooth muscle cells associated with small-diameter branched vessels in *Cxcl12*$^{-/-}$ and *Cxcr4*$^{-/-}$ mutants (Figures 3R versus 3S and 3T, arrowheads; 3U), although smooth muscle coverage in large-diameter veins appeared unaffected (Figures 3R versus 3S and 3T, open arrowheads). Likewise, in *Tie2-Cre; Cxcr4*$^{flox/-}$ mutants, we detected a marked reduction of arterial marker expression (Figures 4C versus 4D, arrowheads; 4E) and smooth muscle coverage (Figures 4H versus 4I, arrowheads; 4J). Taken together, these data indicate that defects in the nerve-vessel alignment observed in *Cxcl12*$^{-/-}$ and *Cxcr4*$^{-/-}$ mutants are accompanied by impaired arterial differentiation and smooth muscle coverage.

We next examined whether Cxcr7, another high affinity receptor for Cxcl12, also has an effect on nerve-vessel alignment and arterial differentiation. Early studies demonstrated that Cxcr7 may modulate or fine-tune the activation of Cxcr4 in response to Cxcl12 (Raz and Mahabaleshwar, 2009). Gross inspection of limb skin vasculature in *Cxcr7*$^{-/-}$ mutants showed that vascular remodeling appeared unaffected (Supplemental Figures S4C versus S4D, arrowheads) and most remodeled vessels aligned with nerves (Supplemental Figures S4A versus S4B, open arrows and arrowheads). Innervation accompanied by BFABP$^+$ migrating Schwann cells appeared normal in the mutants (Supplemental Figures S4F versus S4G, S4H versus S4I, arrows; S4J). However, some smaller vessel branches failed to associate with nerves (Supplemental Figures S4B and S4D, arrows and open arrowheads) demonstrating that *Cxcr7*$^{-/-}$ mutants have less nerve-associated vessel branches than their control littermates (Supplemental Figure S4E). Since *Cxcl12*$^{-/-}$ or *Cxcr4*$^{-/-}$ mutants display more severe defect in nerve-vessel alignment than *Cxcr7*$^{-/-}$ mutants, the loss of Cxcl12-Cxcr4 signaling in endothelial cells primarily influences the fidelity with which remodeled vessel branches align with nerves. We further examined whether the loss of Cxcr7 expression affects arterial differentiation and smooth muscle coverage. No evident attenuation of arterial marker expression was observed in *Cxcr7*$^{-/-}$ mutants (Supplemental Figures S4M versus S4N, arrowheads; S4O). Smooth muscle cell coverage of remodeled small-diameter arteries and large-diameter veins also appeared to be normal in the mutants (Supplemental Figure S4R versus S4S, arrowheads; S4T). Considering our observation that the defects in nerve-vessel alignment and arteriogenesis in *Cxcl12*$^{-/-}$ and *Cxcr4*$^{-/-}$ mutants are fully penetrant, Cxcr7 signaling may not be required for proper arterial differentiation and smooth muscle coverage.

Cxcl12-Cxcr4 signaling does not directly control arterial differentiation

We next considered whether the loss of Cxcl12-Cxcr4 signaling perturbs both nerve-vessel association and arterial differentiation. Our previous studies demonstrated that nerve-derived VEGF-A is required to induce arteriogenesis but not nerve-vessel alignment (Mukouyama et al., 2005). To examine whether Cxcl12 can induce arterial differentiation with or without the addition of VEGF-A, we turned to *in vitro* culture experiments using FACS-purified endothelial cells. As previously described (Mukouyama et al., 2005; Mukouyama et al., 2002), we isolated ephrinB2$^-$, PECAM-1$^+$ endothelial cells from *ephrinB2*$^{taulacZ/+}$ embryos and cultured the cells in the presence of bFGF to support cell survival (Figure 5A). Addition of VEGF-A$_{164}$ to the culture media induced expression of *ephrinB2-taulacZ* (Figure 5B). In contrast, Cxcl12 alone did not up-regulate *ephrinB2-taulacZ* expression at any concentration tested (Figure 5B, 100~900 ng/ml, data not shown). Furthermore, VEGF-A$_{164}$ plus Cxcl12 did not lead to arterial differentiation with synergistic kinetics (Figure 5B). Both factors did not affect cell survival or cell proliferation (Figure 5C, 5E, 5G). Thus, these data indicated that Cxcl12 may not direct arterial differentiation in the limb skin.

Because Cxcr4 expression was detected in a subset of endothelial cells in the limb skin vasculature (Figures 1E and 1G, arrowheads), we sought to further sub-fractionate ephrinB2$^-$, PECAM 1$^+$ endothelial cells by Cxcr4 expression and examine whether

ephrinB2$^-$, PECAM 1$^+$, Cxcr4$^+$ endothelial cells might up-regulate arterial marker expression in response to Cxcl12. Similarly, VEGF-A_{164} strongly enhanced eprhinB2 expression in both Cxcr4$^+$ and Cxcr4$^-$ endothelial cells (Figures 5D and 5F). However, Cxcl12 did not up-regulate ephrinB2 expression in the Cxcr4$^+$ endothelial cells (Figure 5D).

These data indicate that Cxcl12-Cxcr4 signaling does not induce arterial differentiation. To further examine whether Cxcl12-Cxcr4 signaling is required for responsiveness to VEGF-A in endothelial cells, we isolated ephrinB2$^-$, PECAM-1$^+$ endothelial cells from *Cxcr4*$^{-/-}$ mutant embryos using anti-ephrinB2 antibody and cultured the cells in the presence of VEGF-A_{164}. VEGF-A_{164} can induce ephrinB2 expression in *Cxcr4* deficient endothelial cells (Supplemental Figures 5A-5D). These data indicate that Cxcl12-Cxcr4 signaling is not responsible for responsiveness to VEGF-A in arterial differentiation. We next examined whether deficient Cxcl12-Cxcr4 signaling somehow leads to impaired VEGF-A expression in the nerves. There was no significant difference in VEGF-A expression between *Cxcl12*$^{-/-}$ mutants and control littermates (Figures 5H versus 5I, 5J versus 5K, arrows), indicating that defective arterial differentiation in *Cxcl12*$^{-/-}$ or *Cxcr4*$^{-/-}$ mutants is not caused by the reduction of nerve-derived VEGF-A. Considering our previous observation of defective arteriogenesis in mouse mutants lacking *Vegf-a* in nerves, VEGF-A signaling is central to arteriogenesis (Mukouyama et al., 2005). These observations raised the interesting possibility that nerve-derived Cxcl12 directs the nerve-vessel association, and only nerve-associated vessels undergo arteriogenesis via nerve-derived VEGF-A. In this scenario, the loss of Cxcl12-Cxcr4 signaling may perturb arterial differentiation of small-diameter vessels due to their lack of close proximity to the nerves.

Nerve-derived Cxcl12 stimulates endothelial cell migration via Cxcr4

The foregoing experiments indicated that although loss of Cxcl12-Cxcr4 signaling caused a failure of nerve-vessel alignment, it was not directly involved in arterial differentiation. Since endothelial cell migration may be critical during the alignment process, we next examined whether peripheral nerve-derived signal(s) induce endothelial cell migration *in vitro*. To do so, we employed a modified transwell assay using MSS31 cells, a mouse endothelial cell line in which cell surface Cxcr4 expression was detected by flow cytometry (data not shown) and VEGF-A_{164} can enhance arterial differentiation in culture (Supplemental Figures 6A and 6B). DRG were dissociated from E13.5 embryos and cultured for 1-week to produce DRG-conditioned medium (Figure 6A). The DRG conditioned medium was then added to the bottom wells of a multiwell chamber (Figure 6A). MSS31 endothelial cells were added to the upper wells separated from the lower ones by a fibronectin-coated 8 μm porous polycarbonate membrane filter (Figure 6A). Compared to the basic growth medium, we observed that DRG-conditioned medium could induce the migration of MSS31 endothelial cells (Figure 6B). We next examined whether Cxcl12 could induce endothelial cell migration. Interestingly, induction of migration was observed by recombinant Cxcl12 at 300 ng/ml, and the observed effect of Cxcl12 was nearly as strong as that of the DRG-conditioned medium (Figure 6B). Importantly, the migration of endothelial cells elicited by the DRG-conditioned medium was abolished by treating the cells with either anti-Cxcr4 blocking antibody or AMD3100, a selective antagonist for Cxcr4 (Figure 6B; Hatse et al., 2002). Accordingly, the conditioned medium from *Cxcl12* knock-down DRGs (Figure 6C) failed to induce the migration of endothelial cells (Figure 6D). Although VEGF-A_{164} stimulates the migration of endothelial cells (Figure 6F, left), VEGF-A_{164} is not responsible for the chemotactic effect of DRG-conditioned medium on endothelial cell migration (Figure 6F, right). These data strongly suggest that Cxcl12-Cxcr4 signaling mediates the chemotactic effect of DRG-conditioned medium on endothelial cell migration.

Cxcr4 is a seven pass-transmembrane G-protein-coupled receptor (GPCR), which is coupled with pertussis toxin (PTX)-sensitive heterotrimeric G proteins of the G_i family (reviewed in

Dorsam and Gutkind, 2007). We therefore examined whether the migration of MSS31 endothelial cells was sensitive to PTX treatment. Indeed, treatment of MSS31 endothelial cells with PTX resulted in a dramatic inhibition of the migratory response toward both DRG-conditioned medium and Cxcl12 (Figures 6E). These data suggest that G_i protein-mediated Cxcr4 signaling is central to endothelial cell migration stimulated by DRG-conditioned medium.

These findings reveal that during the nerve-vessel alignment process, nerve-derived Cxcl12 instructs the migration of $Cxcr4^+$ endothelial cells to form nerve-associated vessels. Cxcl12-Cxcr4 signaling functions as a long-range chemotactic guidance cue to recruit vessels to align with nerves. Subsequently, nerve-derived VEGF-A instructs arterial differentiation in the nerve-associated vessels. Arterial differentiation presumably requires a local-action of VEGF-A to induce arterial marker expression (Figure 7).

DISCUSSION

Patterning of blood vessel branching is complex and variable, but it is not at all random. In the limb skin, arterial branching is precisely controlled by the branching pattern of peripheral nerves. Nerves provide signals that determine both the pattern of blood vessel branching and arterial differentiation. Our previous studies demonstrated that nerve-derived VEGF-A controls arterial differentiation but not nerve-vessel alignment (Mukouyama et al., 2005; Mukouyama et al., 2002). This highlighted the undetermined nature of the nerve-derived signal that controls the vascular branching pattern during the alignment process. In this study, we have found that nerve-vessel alignment depends on the activity of a GPCR signaling pathway that is mediated by nerve-derived ligand Cxcl12 and its endothelial cell receptor, Cxcr4. Genetic inactivation of Cxcl12-Cxcr4 signaling perturbs nerve-vessel alignment, and abolishes arteriogenesis. Further *in vitro* assays allow us to uncouple nerve-vessel alignment and arteriogenesis revealing that nerve-derived Cxcl12 recruits vessels to nerves and nerve-derived VEGF-A induces arterial differentiation. Our findings, therefore, have revealed a sequential mechanism underlying nerve-mediated patterning and the differentiation processes of endothelial cells.

Cxcl12 as the nerve-mediated vascular patterning signal

Our results support the conclusion that Cxcl12-Cxcr4 signaling controls nerve-mediated arterial branching in developing limb skin. Peripheral nerves express Cxcl12, whereas its receptor Cxcr4 is expressed by a subset of endothelial cells in capillary vessels adjacent to nerves prior to vascular remodeling, and subsequently the expression is restricted to larger nerve-associated arteries. Nerve or Schwann cell-derived Cxcl12 seems diffusible because it can influence endothelial cells in neighboring capillary vessels. Our previous genetic studies provided evidence that Schwann cells produce local signals that control nerve-vessel alignment and arterial differentiation. The loss of *erbB3* receptor signaling *in vivo* results in the complete absence of peripheral nerve-associated Schwann cells, and nerve-vessel alignment and arterial marker expression are greatly reduced (Mukouyama et al., 2002). Because erbB3 expression is not detectable in skin endothelial cells, the vascular defects are likely due to the absence of Schwann cells. To confirm whether Schwann cell-derived Cxcl12 controls nerve-vessel association *in vivo*, a Schwann cell-specific knockout of *Cxcl12* would be required.

Our results imply that nerve-derived Cxcl12 triggers the migration of $Cxcr4^+$ endothelial cells, acting as the nerve-derived chemoattractant signal. Once the $Cxcr4^+$ cells are recruited to the nerve, nerve-derived VEGF-A, but not Cxcl12, influences the cells to induce arterial differentiation. Based on these results, we propose a model in which these two mechanisms underlie the endothelial cell patterning and arterial differentiation during the vascular

remodeling, resulting in the formation of nerve-artery alignment (Figure 7). Because Cxcl12 and VEGF-A are secreted by nerves, the question arises as to how capillary endothelial cells respond to these factors. Perhaps Cxcl12 functions as a long-range chemotactic guidance cue for endothelial cells as shown in other cellular systems: lymphocyte recruitment at sites of immune and inflammatory reactions, primordial germ cell migration and metastatic migration of breast cancer cells towards Cxcl12 expressing organs such as lung, liver and bone marrow (reviewed in Raz and Mahabaleshwar, 2009). On the other hand, arterial differentiation presumably requires local action of VEGF-A in endothelial cells in close proximity to nerves. VEGF-A is secreted as multiple isoforms, which differ in their affinity for heparin in the extracellular matrix. In addition, the VEGF-A co-receptor Nrp1 is preferentially expressed in arterial endothelial cells (Mukouyama et al., 2005; Mukouyama et al., 2002), and is selective for the heparin-binding isoforms (e.g. $VEGF_{164}$) of VEGF-A. Previous studies demonstrated that Nrp1 is required to amplify the VEGF-A effect during arterial differentiation (Mukouyama et al., 2005). Although sensory neurons and glia contribute to the expression of multiple VEGF-A isoforms, the nerve-associated endothelial cells might potentially be exposed to higher levels of Nrp1-binding VEGF-A.

Cxcr4 is the major receptor for Cxcl12-mediated nerve-vessel alignment

The present *loss-of-function* data indicating that *Cxcl12*$^{-/-}$ mutants exhibit an almost identical phenotype to the *Cxcr4*$^{-/-}$ mutation suggest that ligand-receptor interactions between Cxcl12 and Cxcr4 are essential for neuro-vascular associations in the skin. Given that another high affinity receptor, Cxcr7, is involved in cardiac valve development in mice (Gerrits et al., 2008; Sierro et al., 2007; Yu et al., 2011) and Cxcr4-mediated migration of primordial germ cell and posterior lateral line primordium in zebrafish (reviewed in Raz and Mahabaleshwar, 2009), the slight reduction of nerve-vessel alignment seen in *Cxcr7* mutants might be caused by the lack of Cxcr7-mediated fine-tuning of Cxcr4 activation or a Cxcl12 gradient. However, the attenuation has no impact on arterial differentiation. These data suggest that Cxcl12-Cxcr4 signaling is the predominant functional signaling pathway in this system.

Our extensive immunohistochemical analysis of Cxcr4 expression in developing limb skin vasculature reveals that Cxcr4 is expressed by a subset of endothelial cells (16.5% of PECAM-1^{+} endothelial cells are positive for Cxcr4) in capillary vessels before nerve-vessel alignment occurs, and subsequently the expression becomes restricted to nerve-associated arteries. Recent studies indicate that Cxcr4 is expressed by actively sprouting endothelial cells known as tip cells in retina vasculature in the mouse (Strasser et al., 2010). This implies that endothelial Cxcr4 expression in capillary vessels may represent an active phase of cell migration, although no typical tip cell structure is detectable in limb skin capillaries (W.L. and Y.M., unpublished).

This selective expression of Cxcr4 poses the question of whether Cxcr4^{+} endothelial cells are pre-specified to undergo arterial differentiation. Our RT-PCR experiments indicate that the expression of markers of arterial and venous identity does not differ markedly between Cxcr4^{+} and Cxcr4^{-} capillary endothelial cells (Supplemental Figures S1C and S1D). These data suggest that Cxcr4^{+} endothelial cells may not initially be biased towards an arterial fate. If Cxcr4^{+} endothelial cells are committed to arterial fate but have not yet differentiated, then these cells would be fully responsive to VEGF-A in our *in vitro* arterial differentiation assay. Indeed, at most, only 45% of Cxcr4^{+} endothelial cells underwent arterial differentiation, and there appeared to be no significant difference in the effect of VEGF-A between Cxcr4^{+} and Cxcr4^{-} endothelial cells. Taken together, we cannot presently discern whether Cxcr4 expression in capillary endothelial cells is correlated with commitment to an arterial fate.

Cxcl12 and VEGF-A as hypoxia-inducible genes

How are the expression of Cxcl12 and VEGF-A coordinated in nerves? One scenario is that oxygen-starved nerves produce local signals that govern the precise pattern of arterial branching along with the nerves during angiogenic remodeling. In support of this, it has been reported that hypoxia induces Cxcl12 and VEGF-A expression through activation of the transcription factor hypoxia-inducible factor-1 (HIF-1) (Ceradini et al., 2004; Forsythe et al., 1996; Shweiki et al., 1992). Previous studies have indicated that the induction of VEGF-A and Cxcl12 in response to hypoxia/ischemia promotes neovascularization with tumor progression (Plate et al., 1992) and tissue regeneration (Ceradini et al., 2004), suggesting that expression of these signals is common. Local hypoxia may trigger Cxcl12 and VEGF-A expression in the nerves, directing arterial branching along the nerves during vascular remodeling. Since the regulatory regions of *Cxcl12* and *Vegf-a* genes contain a HIF-dependent hypoxia-responsive enhancer, a direct test of this scenario will require nerve-specific knockouts of *Hif-1*.

Organ-specific vascular patterning

Blood flow is critical for the processes in which a primary capillary plexus undergoes extensive vascular remodeling and develops into a hierarchical branched, vascular network (Culver and Dickinson, 2010). However, hemodynamic force alone is not sufficient to establish a highly stereotypical vascular branching pattern or determine arterial and/or venous fate in an organ-specific manner. As such, the embryonic limb skin vasculature model has proven to be useful for studying how organ-specific local signals provided by organized components such as nerves, coordinate vascular remodeling and the formation of branched arterial networks. Two different mechanisms underlying endothelial cell migration induced by Cxcl12 and arterial differentiation induced by VEGF-A, act in concert resulting in nerve-artery alignment. Similar coordinated action may be observed in various organs, where different components secrete these signals to develop organotypic patterns of arterial branching.

EXPERIMENTAL PROCEDURES

Experimental animals

The characterization of *Cxcl12*$^{-/-}$ mice (Nagasawa et al., 1996), *Cxcr4*$^{-/-}$ mice (Tachibana et al., 1998), *Cxcl12*$^{GFP/+}$ knock-in mice (Ara et al., 2003), *Cxcr4*$^{flox/-}$ mice (Tokoyoda et al., 2004), *Tie2-Cre* mice (Ara et al., 2005; Kisanuki et al., 2001), *ephrinB2*$^{taulacZ/+}$ mice (Wang et al., 1998), and *Sema3A*$^{-/-}$ mice (Taniguchi et al., 1997) have been reported elsewhere. Conventional *Cxcr7* knockout mice were generated at the Zou laboratory by homologous recombination in ES cells according to standard procedures.

RT-PCR

Quantitative mRNA expression analysis of chemokines and their receptors in E13.5 DRG and forelimbs was performed with the mouse chemokine and receptor RT^2 profiler PCR array (QIAGEN) on 7500 Real Time PCR systems (Applied Biosystems) using RT^2 SYBR Green qPCR master mix (QIAGEN). A detailed description of experiments and the sequence of the PCR primers are described in the SUPPLEMENTAL EXPERIMENTAL PROCEDURES.

Whole-mount immunohistochemistry of limb skin

Staining was performed essentially as described previously (Mukouyama et al., 2002; Li and Mukouyama, 2011). All confocal microscopy was carried out on a Leica TCS SP5 confocal (Leica). The average mean fluorescence (pixel/area) and nerve length were analyzed using

NIH ImageJ software (NIH). Vascular density (volume of vessels per Mm^3) was analyzed using Volocity software (PerkinElmer). Number of embryos is indicated as "n" in FIGURE LEGENDS. Statistic significance of samples was assessed using Student's *t*-test. Details of the procedure are available in the SUPPLEMENTAL EXPERIMENTAL PROCEDURES.

Section immunohistochemistry

Section staining was performed as described previously (Mukouyama et al., 2005). All confocal microscopy was carried out on a Leica TCS SP5 confocal (Leica). H&E staining of sections was performed and images were captured using QImaging RETIGA 2000R camera (QImaging). Details of the procedure are available in the SUPPLEMENTAL EXPERIMENTAL PROCEDURES.

Flow cytometry and culture methods

Forelimb skins were peeled off from E13.5 and E15.5 embryos and dissociated by digestion with 1 mg/ml type I collagenase (Worthington), 3mg/ml Dispase (Gibco/Invitrogen) and 0.5mg/ml deoxyribonuclease type 1 (DNase 1; Sigma). The dissociated cells were then stained with PE-conjugated anti-PECAM-1 antibody (1:50, BD Pharmingen, 30 min on ice) and/or APC-conjugated anti-Cxcr4 antibody (1:50, BD Pharmingen, 30 min on ice). The PECAM 1^+, $Cxcr4^+$ population was sorted into Trizol Reagent (Invitrogen) for total RNA preparation. All cell sorts and analyses were performed on a MoFlo (Beckman Coulter, Fort Collins, CO.). Details of the procedure for the isolation and culture of ephrinB2-negative, eprhinB2-negative Cxcr4 positive or ephrinB2 negative Cxcr4 negative endothelial cells from E11.5 *ephrinB2*$^{lacZ/+}$ embryos are available in the SUPPLEMENTAL EXPERIMENTAL PROCEDURES.

DRG isolation and culture methods

DRG were isolated from E13.5 embryos as previously described (Mukouyama et al., 2002). Briefly, DRG were dissociated by digestion with a Papain Dissociation System (Worthington). Culture medium contains EGM-2 MV (Lonza) with SingleQuots supplement (Lonza). The freshly isolated cells were cultured or infected by CXCL12 shRNA lentivirus (3TU/cell, Sigma) with 25 ng/ml NGF (UBI) on fibronectin (Biomedical Technologies) coated dishes for 7 days, and the supernatant was passed through a 0.45μm filter after centrifugation.

Chemotactic migration assay

Chemotactic migration assay was performed with a 48-well modified Boyden chamber (NeuroProbe) using a polycarbonate membrane with a 8 μm pore size. Details of the procedure are available in the SUPPLEMENTAL EXPERIMENTAL PROCEDURES.

Supplementary Material

Refer to Web version on PubMed Central for supplementary material.

Acknowledgments

We thank X. Chi and F. Costantini for breeding *Cxcr7* mutants, A. L. Kolodkin for providing anti-Nrp1 antibody, T. Müller for providing anti-BFABP antibody, M. Taniguchi for providing *Sema3A* mutants and N. Takakura for providing anti-ephrinB2 antibody. Thanks to L. Samsel, P. Dagur, H. Mariani and P. J. McCoy for FACS assistance, and J. Hawkins and the staff of NIH Bldg50 animal facility for assistance with mouse breeding and care, K. Gill for laboratory management and technical support, and Y. Carter and L. Oundo for administrative assistance. Thanks also to A. M. Michelson, R. S. Balaban, R. S. Adelstein, S. Gutkind and H. Yagi for invaluable help and discussion, H. Zang and M. A. Conti for editorial advice on the manuscript, and other members of Laboratory of Stem Cell and Neuro-Vascular Biology for technical help and thoughtful discussion. None of the authors has any

financial or other conflicts of interests. This work was supported by the Intramural Research Program of the National Heart, Lung, and Blood Institute, National Institutes of Health.

REFERENCES

Adams RH, Eichmann A. Axon guidance molecules in vascular patterning. Cold Spring Harb Perspect Biol. 2010; 2:a001875. [PubMed: 20452960]

Ara T, Tokoyoda K, Okamoto R, Koni PA, Nagasawa T. The role of CXCL12 in the organ specific process of artery formation. Blood. 2005; 105:3155–3161. [PubMed: 15626744]

Ara T, Tokoyoda K, Sugiyama T, Egawa T, Kawabata K, Nagasawa T. Long-term hematopoietic stem cells require stromal cell-derived factor-1 for colonizing bone marrow during ontogeny. Immunity. 2003; 19:257–267. [PubMed: 12932359]

Argraves WS, Drake CJ. Genes critical to vasculogenesis as defined by systematic analysis of vascular defects in knockout mice. The anatomical record Part A, Discoveries in molecular, cellular, and evolutionary biology. 2005; 286:875–884.

Ceradini DJ, Kulkarni AR, Callaghan MJ, Tepper OM, Bastidas N, Kleinman ME, Capla JM, Galiano RD, Levine JP, Gurtner GC. Progenitor cell trafficking is regulated by hypoxic gradients through HIF-1 induction of SDF-1. Nat Med. 2004; 10:858–864. [PubMed: 15235597]

Cha YR, Fujita M, Butler M, Isogai S, Kochhan E, Siekmann AF, Weinstein BM. Chemokine signaling directs trunk lymphatic network formation along the preexisting blood vasculature. Dev Cell. 2012; 22:824–836. [PubMed: 22516200]

Coultas L, Chawengsaksophak K, Rossant J. Endothelial cells and VEGF in vascular development. Nature. 2005; 438:937–945. [PubMed: 16355211]

Culver JC, Dickinson ME. The effects of hemodynamic force on embryonic development. Microcirculation. 2010; 17:164–178. [PubMed: 20374481]

Dorrell MI, Friedlander M. Mechanisms of endothelial cell guidance and vascular patterning in the developing mouse retina. Progress in retinal and eye research. 2006; 25:277–295. [PubMed: 16515881]

Dorsam RT, Gutkind JS. G-protein-coupled receptors and cancer. Nature reviews Cancer. 2007; 7:79–94.

Forsythe JA, Jiang BH, Iyer NV, Agani F, Leung SW, Koos RD, Semenza GL. Activation of vascular endothelial growth factor gene transcription by hypoxia-inducible factor 1. Mol Cell Biol. 1996; 16:4604–4613. [PubMed: 8756616]

Gerrits H, van Ingen Schenau DS, Bakker NE, van Disseldorp AJ, Strik A, Hermens LS, Koenen TB, Krajnc Franken MA, Gossen JA. Early postnatal lethality and cardiovascular defects in CXCR7-deficient mice. Genesis. 2008; 46:235–245. [PubMed: 18442043]

Hatse S, Princen K, Bridger G, De Clercq E, Schols D. Chemokine receptor inhibition by AMD3100 is strictly confined to CXCR4. FEBS Lett. 2002; 527:255–262. [PubMed: 12220670]

Kisanuki YY, Hammer RE, Miyazaki J, Williams SC, Richardson JA, Yanagisawa M. Tie2-Cre transgenic mice: a new model for endothelial cell-lineage analysis in vivo. Dev Biol. 2001; 230:230–242. [PubMed: 11161575]

Kurtz A, Zimmer A, Schnutgen F, Bruning G, Spener F, Muller T. The expression pattern of a novel gene encoding brain-fatty acid binding protein correlates with neuronal and glial cell development. Development. 1994; 120:2637–2649. [PubMed: 7956838]

Lawson ND, Vogel AM, Weinstein BM. sonic hedgehog and vascular endothelial growth factor act upstream of the Notch pathway during arterial endothelial differentiation. Dev Cell. 2002; 3:127–136. [PubMed: 12110173]

Li W, Mukouyama YS. Whole-mount Immunohistochemical Analysis for Embryonic Limb Skin Vasculature: a Model System to Study Vascular Branching Morphogenesis in Embryo. J Vis Exp. 2011

Mukouyama YS, Gerber HP, Ferrara N, Gu C, Anderson DJ. Peripheral nerve-derived VEGF promotes arterial differentiation via neuropilin 1-mediated positive feedback. Development. 2005; 132:941–952. [PubMed: 15673567]

Mukouyama YS, Shin D, Britsch S, Taniguchi M, Anderson DJ. Sensory nerves determine the pattern of arterial differentiation and blood vessel branching in the skin. Cell. 2002; 109:693–705. [PubMed: 12086669]

Nagasawa T, Hirota S, Tachibana K, Takakura N, Nishikawa S, Kitamura Y, Yoshida N, Kikutani H, Kishimoto T. Defects of B-cell lymphopoiesis and bone-marrow myelopoiesis in mice lacking the CXC chemokine PBSF/SDF-1. Nature. 1996; 382:635–638. [PubMed: 8757135]

Plate KH, Breier G, Weich HA, Risau W. Vascular endothelial growth factor is a potential tumour angiogenesis factor in human gliomas in vivo. Nature. 1992; 359:845–848. [PubMed: 1279432]

Raz E, Mahabaleshwar H. Chemokine signaling in embryonic cell migration: a fisheye view. Development. 2009; 136:1223–1229. [PubMed: 19304885]

Risau W. Mechanisms of angiogenesis. Nature. 1997; 386:671–674. [PubMed: 9109485]

Shweiki D, Itin A, Soffer D, Keshet E. Vascular endothelial growth factor induced by hypoxia may mediate hypoxia-initiated angiogenesis. Nature. 1992; 359:843–845. [PubMed: 1279431]

Siekmann AF, Standley C, Fogarty KE, Wolfe SA, Lawson ND. Chemokine signaling guides regional patterning of the first embryonic artery. Genes Dev. 2009; 23:2272–2277. [PubMed: 19797767]

Sierro F, Biben C, Martinez-Munoz L, Mellado M, Ransohoff RM, Li M, Woehl B, Leung H, Groom J, Batten M, et al. Disrupted cardiac development but normal hematopoiesis in mice deficient in the second CXCL12/SDF-1 receptor, CXCR7. Proc Natl Acad Sci U S A. 2007; 104:14759–14764. [PubMed: 17804806]

Strasser GA, Kaminker JS, Tessier-Lavigne M. Microarray analysis of retinal endothelial tip cells identifies CXCR4 as a mediator of tip cell morphology and branching. Blood. 2010; 115:5102–5110. [PubMed: 20154215]

Tachibana K, Hirota S, Iizasa H, Yoshida H, Kawabata K, Kataoka Y, Kitamura Y, Matsushima K, Yoshida N, Nishikawa S, et al. The chemokine receptor CXCR4 is essential for vascularization of the gastrointestinal tract. Nature. 1998; 393:591–594. [PubMed: 9634237]

Takabatake Y, Sugiyama T, Kohara H, Matsusaka T, Kurihara H, Koni PA, Nagasawa Y, Hamano T, Matsui I, Kawada N, et al. The CXCL12 (SDF 1)/CXCR4 axis is essential for the development of renal vasculature. Journal of the American Society of Nephrology : JASN. 2009; 20:1714–1723. [PubMed: 19443644]

Taniguchi M, Yuasa S, Fujisawa H, Naruse I, Saga S, Mishina M, Yagi T. Disruption of semaphorin III/D gene causes severe abnormality in peripheral nerve projection. Neuron. 1997; 19:519–530. [PubMed: 9331345]

Tokoyoda K, Egawa T, Sugiyama T, Choi BI, Nagasawa T. Cellular niches controlling B lymphocyte behavior within bone marrow during development. Immunity. 2004; 20:707–718. [PubMed: 15189736]

Visconti RP, Richardson CD, Sato TN. Orchestration of angiogenesis and arteriovenous contribution by angiopoietins and vascular endothelial growth factor (VEGF). Proc Natl Acad Sci U S A. 2002; 99:8219–8224. [PubMed: 12048246]

Wang HU, Chen ZF, Anderson DJ. Molecular distinction and angiogenic interaction between embryonic arteries and veins revealed by ephrin-B2 and its receptor Eph-B4. Cell. 1998; 93:741–753. [PubMed: 9630219]

Yu S, Crawford D, Tsuchihashi T, Behrens TW, Srivastava D. The chemokine receptor CXCR7 functions to regulate cardiac valve remodeling. Dev Dyn. 2011; 240:384–393. [PubMed: 21246655]

HIGHLIGHTS

- Cxcr4 is expressed by a subset of endothelial cells in the capillary network.
- Genetic inactivation of Cxcl12-Cxcr4 signaling perturbs nerve-vessel alignment.
- Cxcl12 controls endothelial migration, while VEGF directs arterial differentiation.

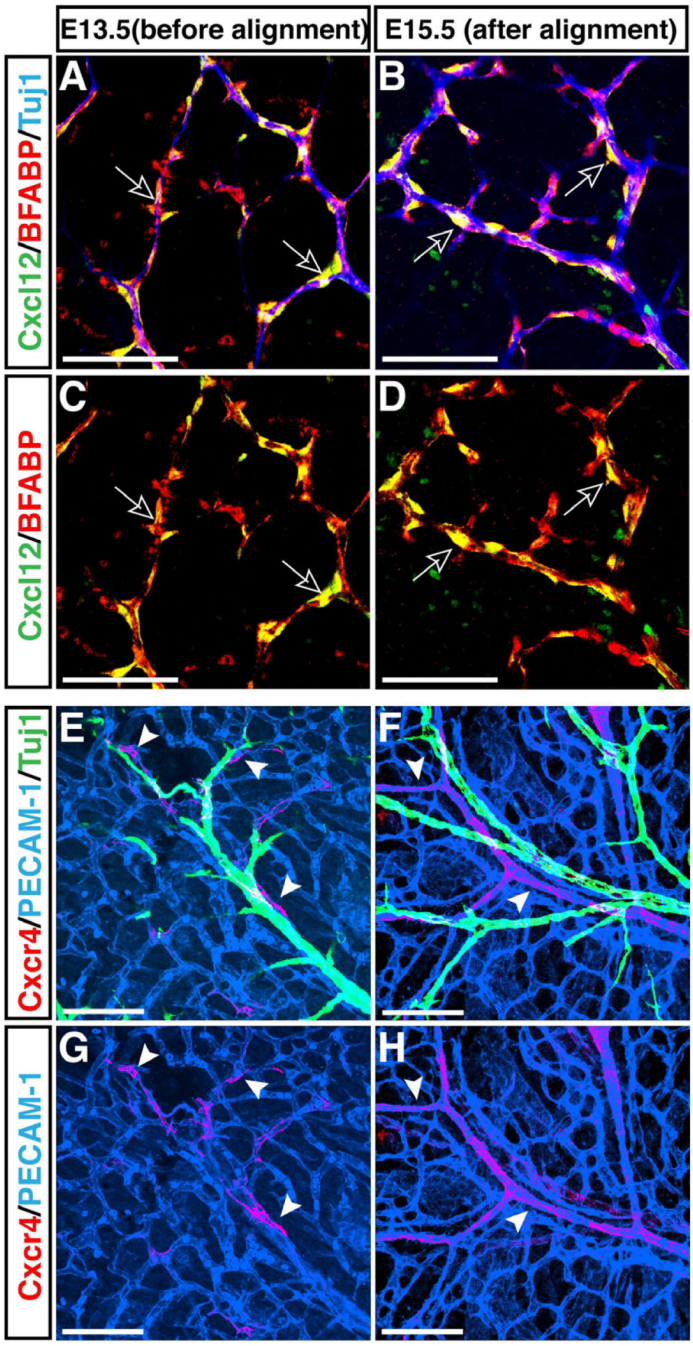

Figure 1. Complementary expression of Cxcl12 and its receptor Cxcr4 in nerves and vessels in the developing limb skin

Whole-mount immunohistochemical analysis of limb skin from E13.5 and E15.5 *Cxcl12*^{GFP} embryos with antibodies to the neuron specific marker βIII tubulin (Tuj1, A and B, blue, and E and F, green), the Schwann cell marker BFABP (A-D, red), the pan-endothelial cell marker PECAM-1 (E-H, blue), Cxcl12 (*Cxcl12*^{GFP}, A-D, green) and Cxcr4 (anti-Cxcr4 antibody from Biotrend, E-H, red) is shown. At E13.5, no association between nerves and capillary vessels was yet evident (E). BFABP^{+} migrating Schwann cells in nerves express Cxcl12 (A and C, open arrows). Cxcr4 expression was detected in a subset of capillary vessels near nerves (E and G, red, arrowheads). By E15.5, vascular remodeling had

occurred, and nerves were associated with arteries (F). Schwann cells continued to express Cxcl12 (B and D, open arrows), whereas Cxcr4 expression was restricted to nerve-associated arteries (F and H, arrowheads). Scale bars are 100 μm.

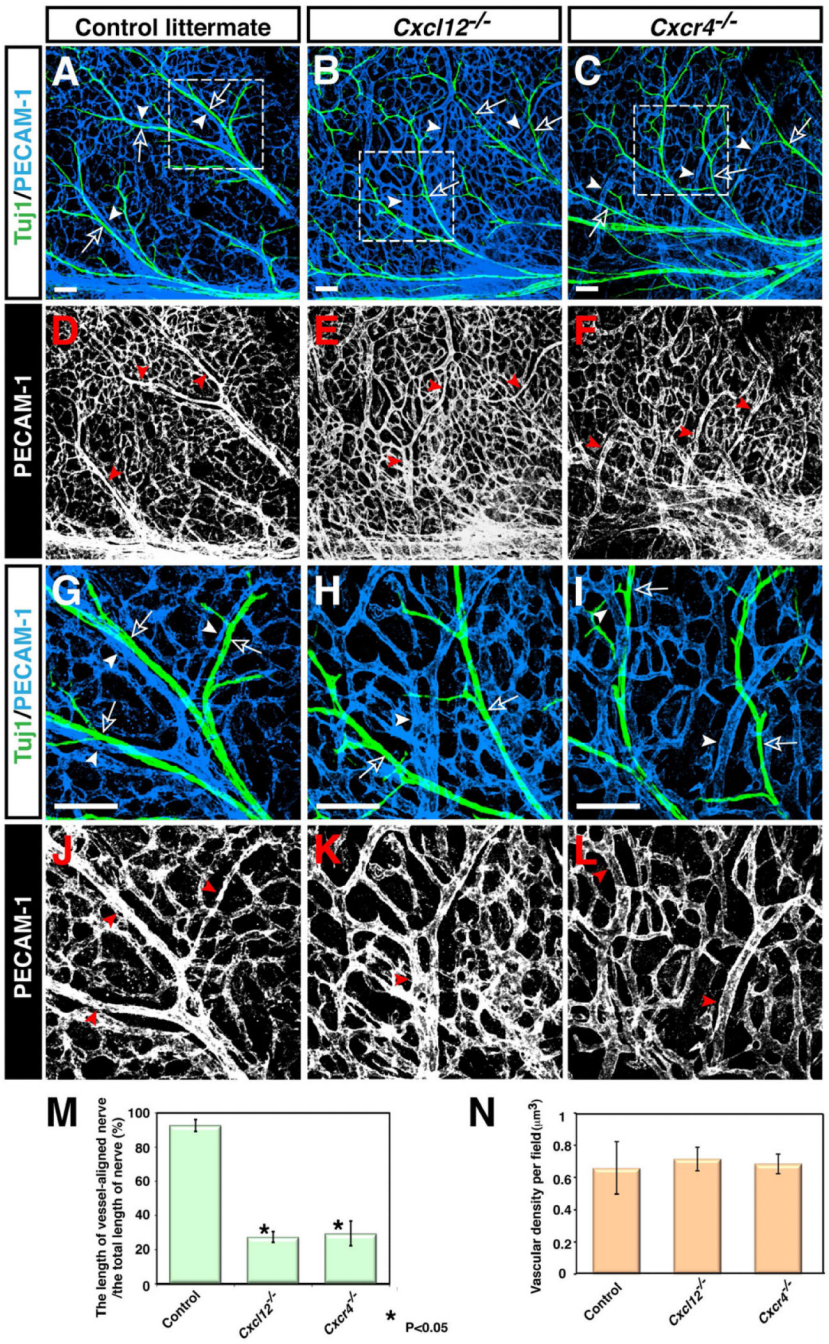

Figure 2. Disruption of nerve-vessel alignment in *Cxcl12* and *Cxcr4* homozygous mutants

Whole-mount double immunofluorescence labeling of limb skin with antibodies to PECAM-1 (A-C and G-I, blue; D-F and J-L, white) and βIII tubulin (Tuj1, A-C and G-I, green) in *Cxcl12*$^{-/-}$ mutants (B, E, H, K), *Cxcr4*$^{-/-}$ mutants (C, F, I, L), or control littermates (A, D, G, J) at E15.5 is shown. Close-up images (G-L) show the boxed regions in A, B, C. Both *Cxcl12*$^{-/-}$ and *Cxcr4*$^{-/-}$ mutants exhibited aberrant patterns of remodeled vessels (B, E, H, K for *Cxcl12*$^{-/-}$ mutants; C, F, I, L for *Cxcr4*$^{-/-}$ mutants, arrowheads), resulting in disruption of nerve-vessel alignment (B, C, H, I, open arrows and arrowheads). Note that branching patterns of Tuj1^{+} nerves are not affected in either homozygous mutant (A-C and G-I, green). (M) Quantification of the nerve-vessel alignment as the percentage of nerve-

length aligned with vessels was performed. *Cxcl12*$^{-/-}$ and *Cxcr4*$^{-/-}$ mutants exhibit defective nerve-vessel alignment. Asterisk indicates statistically significant difference ($P<0.05$) in both mutants compared with control littermates according to Student's *t*-test (n=5 per genotype; bars represent mean ± SEM). (N) Quantification of vascular density in *Cxcl12*$^{-/-}$ and *Cxcr4*$^{-/-}$ mutants compared with control littermates was shown (n=4 per genotype; bars represent mean ± SEM). There was no significant difference in vascular density between *Cxcl12*$^{-/-}$ mutants, *Cxcr4*$^{-/-}$ mutants, and control littermates. Scale bars are 100 μm.

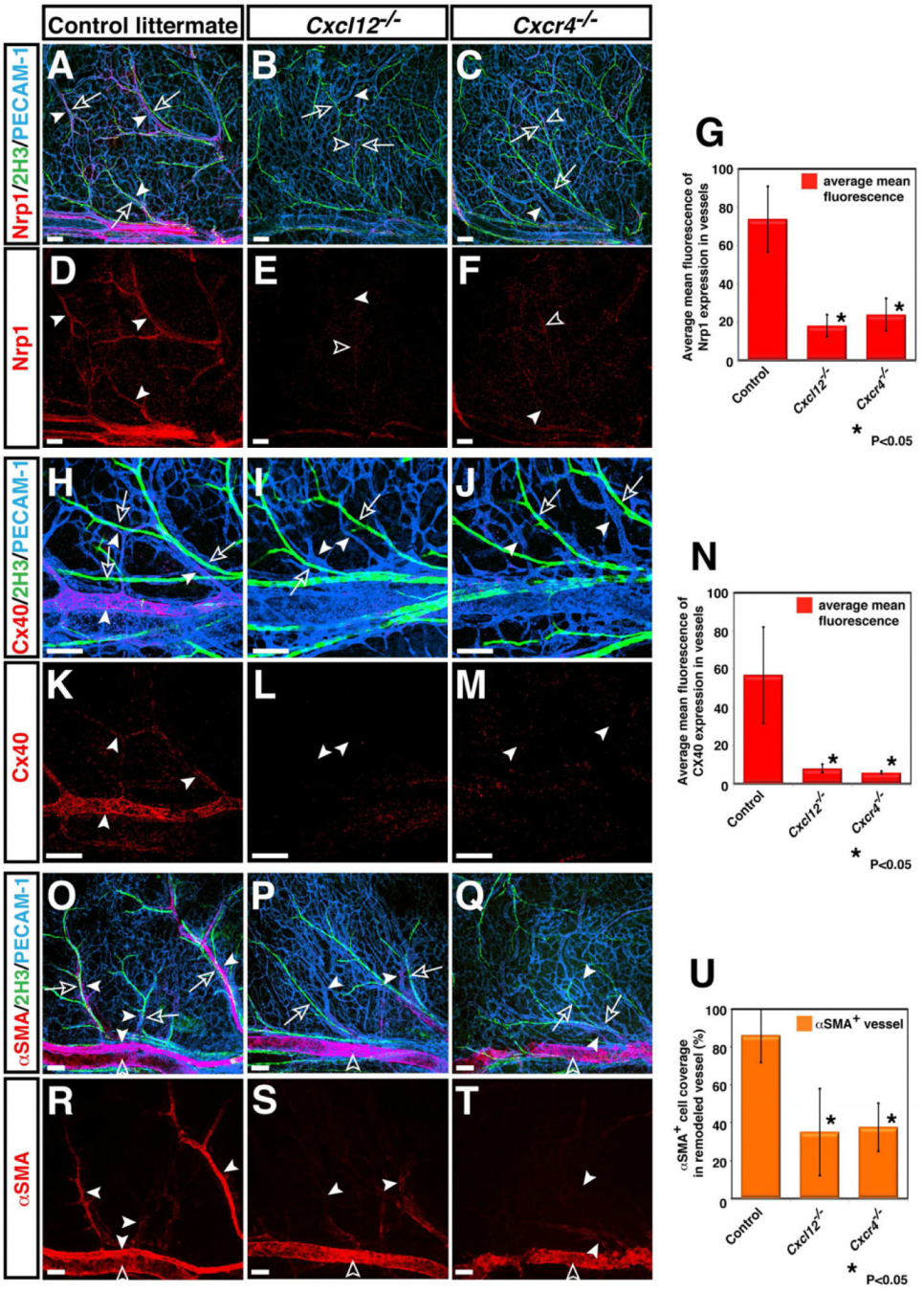

Figure 3. Defective arterial differentiation and smooth muscle coverage in *Cxcl12* and *Cxcr4* homozygous mutants

Whole-mount triple immunofluorescence labeling of limb skin with antibodies to arterial markers either Nrp1 (A-F, red, arrowheads) or Cx40 (H-M, red, arrowheads) and the smooth muscle cell marker αSMA (O-T, red, arrowheads), in addition to PECAM-1 (A-C, H-J and O-Q, blue) and neurofilament (2H3, A-C, H-J and O-Q, green, open arrows) in *Cxcl12*$^{-/-}$ (B, E, I, L, P, S), *Cxcr4*$^{-/-}$ (C, F, J, M, Q, T) or control littermates (A, D, H, K, O, R) at E15.5 is shown. The expression of arterial markers such as Nrp1 and Cx40 was conspicuously reduced in remodeled vessels of both *Cxcl12*$^{-/-}$ and *Cxcr4*$^{-/-}$ mutants (B, C, E, F for Nrp1 expression; I, J, L, M for Cx40 expression, arrowheads). Note that weak Nrp1 expression

can be detected in some remodeled vessels in relatively close proximity to nerves in *Cxcl12*$^{-/-}$ (B, E, open arrowheads) and *Cxcr4*$^{-/-}$ mutants (C, F, open arrowheads). Fewer αSMA^{+} smooth muscle cells associated with small-diameter branched vessels in *Cxcl12*$^{-/-}$ and *Cxcr4*$^{-/-}$ mutants (O versus P and Q, R versus S and T, arrowheads), although smooth muscle coverage in large-diameter veins appeared unaffected (S and T, open arrowheads). Quantification of arterial marker expression (G and N) or αSMA^{+} smooth muscle cell coverage (U) in small-diameter branched vessels was performed (n=4 per genotype; bars represent mean ± SEM). Asterisk indicates statistically significant difference (*P<0.05*) in both mutants compared with control littermates according to Student's *t*-test. Scale bars are 100 μm.

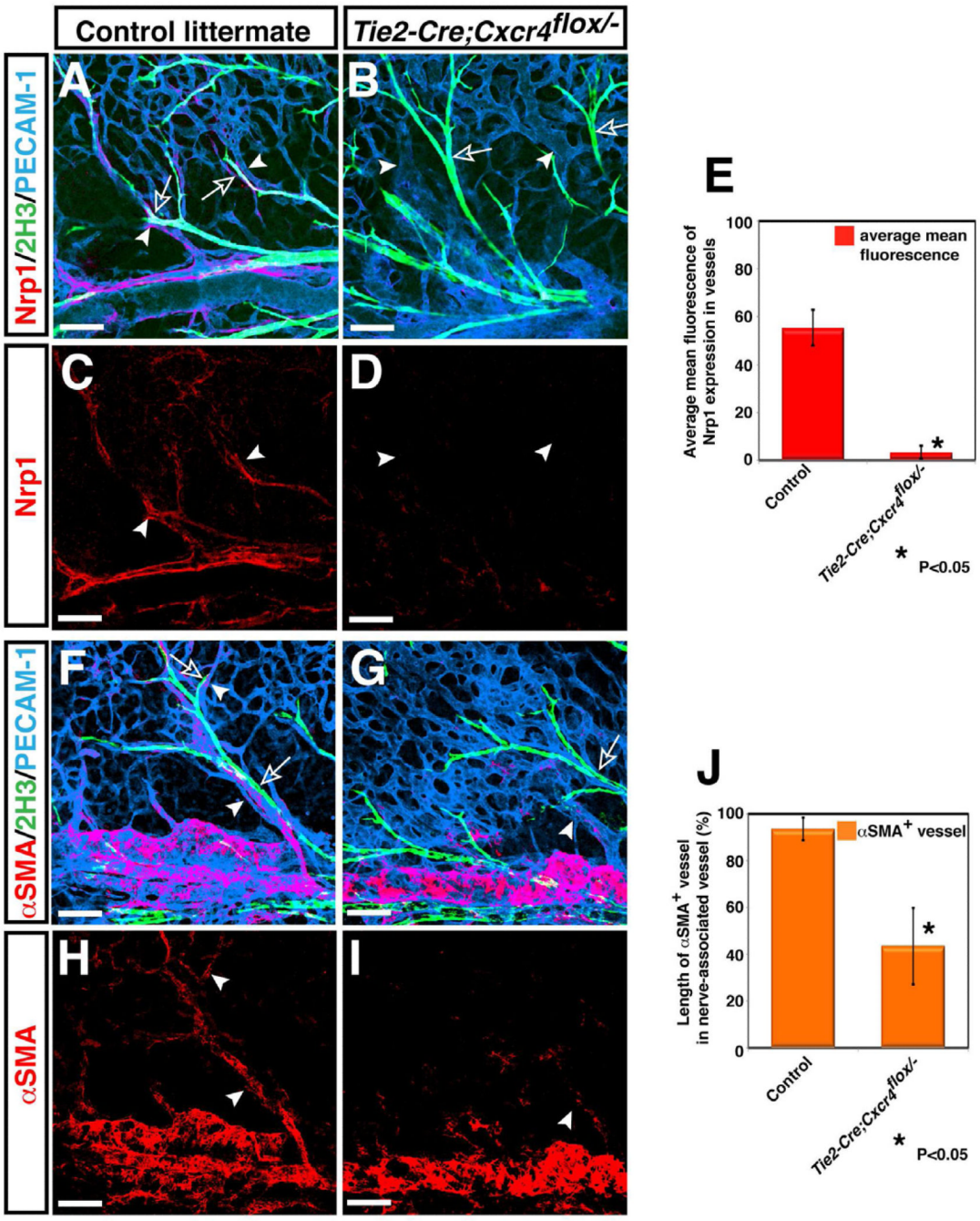

Figure 4. Requirement for endothelial Cxcr4 for patterns of vascular branching and arteriogenesis

Whole-mount triple immunofluorescence labeling of limb skin with antibodies to the arterial marker Nrp1 (A-D, red, arrowheads) and the smooth muscle cell marker αSMA (F-I, red, arrowheads), in addition to PECAM-1 (A, B, F, G, blue) and neurofilament (2H3, A, B, F, G, green, open arrows) in *Tie2-Cre; Cxcr4*$^{flox/-}$ and control littermates is shown. Compared to control littermates, disrupted nerve-vessel alignment was observed in *Tie2-Cre; Cxcr4*$^{flox/-}$ mutants (A versus B, arrowheads and open arrows). The expression of Nrp1 was nearly abolished in *Tie2-Cre; Cxcr4*$^{flox/-}$ mutants (D, arrowheads). αSMA^{+} smooth muscle cell coverage was strongly reduced in small-diameter branched vessels in *Tie2-Cre;*

Cxcr4$^{flox/-}$ mutants (F versus G, H versus I, arrowheads), although smooth muscle coverage in large-diameter veins appeared unaffected (F versus G, H versus I). Overall, *Tie2-Cre; Cxcr4*$^{flox/-}$ mutants exhibit an almost identical phenotype to *Cxcl12*$^{-/-}$ or *Cxcr4*$^{-/-}$ mutants. Quantification of Nrp1 expression (E) or αSMA^{+} smooth muscle cell coverage (J) in small-diameter branched vessels was performed (n=3 per genotype; bars represent mean ± SEM). Asterisk indicates statistically significant difference ($P<0.05$) in mutants compared with control littermates according to Student's *t*-test. Scale bars are 100 μm.

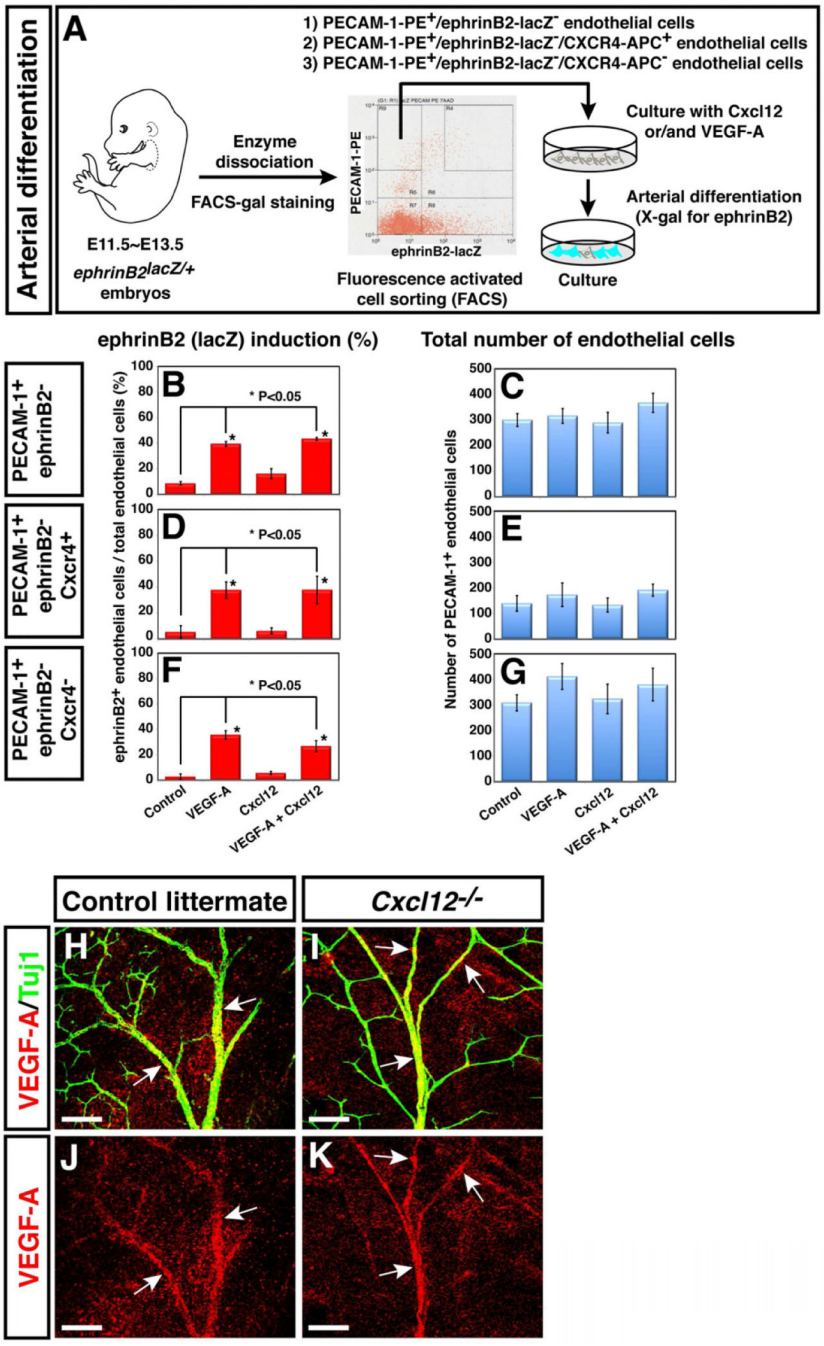

Figure 5. Cxcl12 cannot induce arterial differentiation in vitro

(A) Schematic illustrating the experimental procedure for endothelial cell isolation from E11.5 *ephrinB2*$^{taulacZ/+}$ heterozygous embryos and the arterial differentiation assay in culture. (B-G) PECAM-1^{+}/ephrinB2^{-} (B and C), PECAM-1^{+}/ephrinB2^{-}/CXCR4^{+} (D and E) or PECAM^{-}1^{+}/ephrinB2^{-}/CXCR4^{-} (F and G) endothelial cells were cultured in 10 ng/ml VEGF-A, 500 ng/ml Cxcl12 or both proteins plus 10 ng/ml bFGF for 2 days, followed by double-staining with X-gal and anti-PECAM-1 antibody. Note that VEGF-A induced ephrinB2 expression in ~45% of FACS-purified endothelial cells without change in the total number of endothelial cells. By contrast, Cxcl12 by itself did not up-regulate ephrinB2 expression, and showed no synergistic effect with VEGF-A. Furthermore, no increase of

ephrinB2 expression was observed under these conditions in the $Cxcr4^{+}$ subpopulation of endothelial cells. Statistical analysis is from 3 independent experiments (bars represent mean ± SEM). Asterisk indicates statistically significant difference ($P<0.05$) according to Student's *t*-test. (H-K) Whole-mount immunohistochemical analysis of limb skin with antibodies to VEGF (red, arrows) and βIII tubulin (Tuj1, green) is shown. There was no significant difference in VEGF-A expression between *Cxcl12*$^{-/-}$ mutants (I and K) and control littermates (H and J). Scale bars are 100 μm.

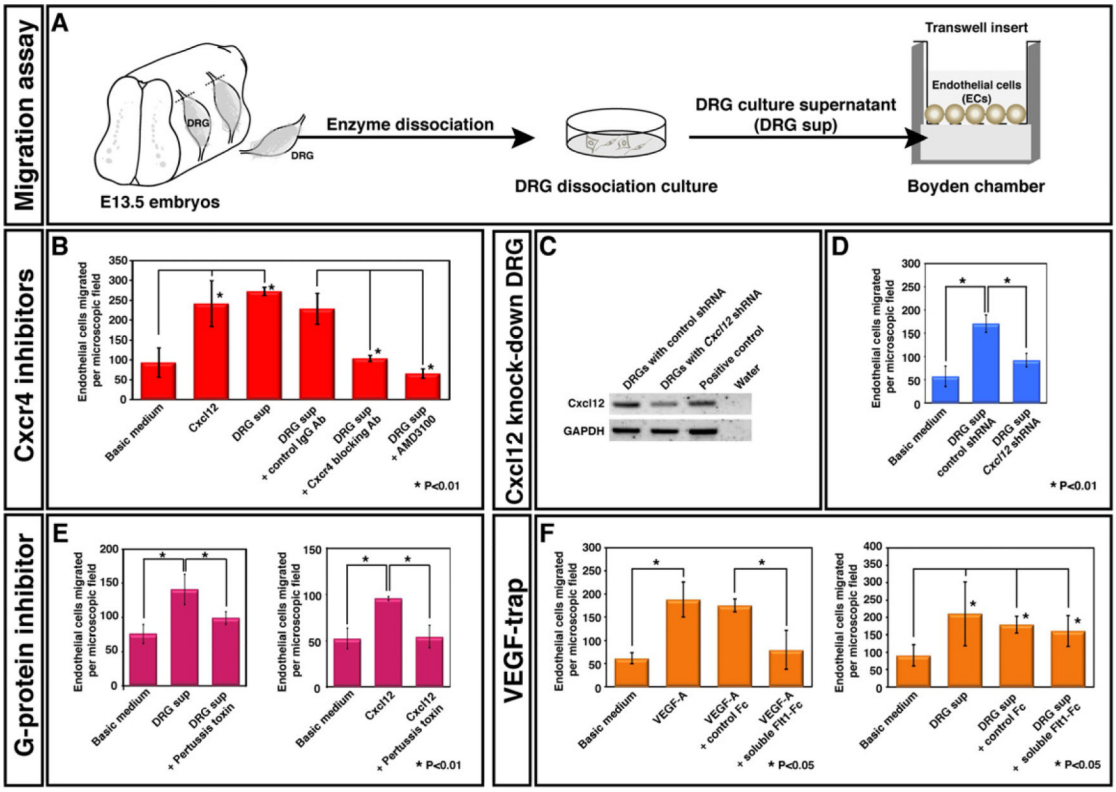

Figure 6. Purified DRG sensory neurons and Schwann cells promote endothelial cell migration in vitro via Cxcl12-Cxcr4 signaling

(A) Schematic illustrating the experimental procedure for DRG dissection from E13.5 embryos and the chemotaxis assay. (B) DRG culture supernatant stimulated migration of Cxcr4^{+} MSS31 endothelial cells and this effect was blocked by treatment with either anti-Cxcr4 blocking antibody (R&D) or AMD3100, a selective antagonist for Cxcr4. 300 ng/ml Cxcl12 stimulated migration of MSS31 endothelial cells at a level similar to the DRG culture supernatant. Statistical analysis is from 3 independent experiments (bars represent mean ± SEM). Asterisks indicate statistically significant induction of migration of MSS31 endothelial cells ($p<0.01$) after treatment with Cxcl12 or the DRG culture supernatant, and statistically significant inhibition of DRG-supernatant stimulated migration of MSS31 endothelial cells ($p<0.01$) after treatment with anti-Cxcr4 blocking antibody or AMD3100, according to a Student's *t*-test. (C and D) The supernatant from *Cxcl12* knock-down DRG culture failed to induce migration of MSS31 endothelial cells. DRGs were infected with a control or *Cxcl12* shRNA lentivirus. The expression levels of *Cxcl12* were assessed by RT-PCR analysis (C). Compared to the supernatant from control shRNA-treated DRG culture, the supernatant from *Cxcl12* knock-down DRG culture failed to induce migration of MSS31 endothelial cells. Statistical analysis is from 3 independent experiments (bars represent mean ± SEM). Asterisks indicate statistically significant induction of migration of MSS31 endothelial cells ($P<0.01$) after treatment with the supernatant from control shRNA-treated DRG culture, and statistically significant reduction of migration of MSS31 endothelial cells ($P<0.01$) after treatment with the supernatant from *Cxcl12* knock-down DRG culture, according to a Student's *t*-test. (E) The effect on endothelial cell migration induced by the DRG culture supernatant or 300ng/ml Cxcl12 was blocked by treatment with 2ng/ml Pertussis toxin, a G-protein inhibitor. Statistical analysis is from 3 independent experiments (bars represent mean ± SEM). Asterisk indicates statistically significant difference (P<0.01) according to Student's t-test. (F) VEGF-A is not responsible for the effect on endothelial cell

migration induced by the DRG culture supernatant. 10ng/ml VEGF-A stimulated migration of MSS31 endothelial cells and this effect was blocked by treatment with 100 ng/ml soluble Flt1-Fc (VEGFR1-Fc) protein. 100ng/ml soluble Flt1-Fc protein failed to block DRG-supernatant stimulated migration of MSS31 endothelial cells. Statistical analysis is from 3 independent experiments (bars represent mean ± SEM). On the left panel, asterisks indicate statistically significant induction of migration of MSS31 endothelial cells ($p<0.05$) induced by treatment with VEGF-A, and statistically significant inhibition of VEGF-A stimulated migration of MSS31 endothelial cells ($p<0.01$) after treatment with soluble Flt1-Fc protein compared to control Fc protein, according to a Student's *t*-test. On the right panel, asterisks indicate statistically significant induction of migration of MSS31 endothelial cells ($p<0.05$) induced by treatment with the DRG culture supernatant with or without control Fc protein or soluble Flt1-Fc protein compared to basic medium, according to a Student's *t*-test.

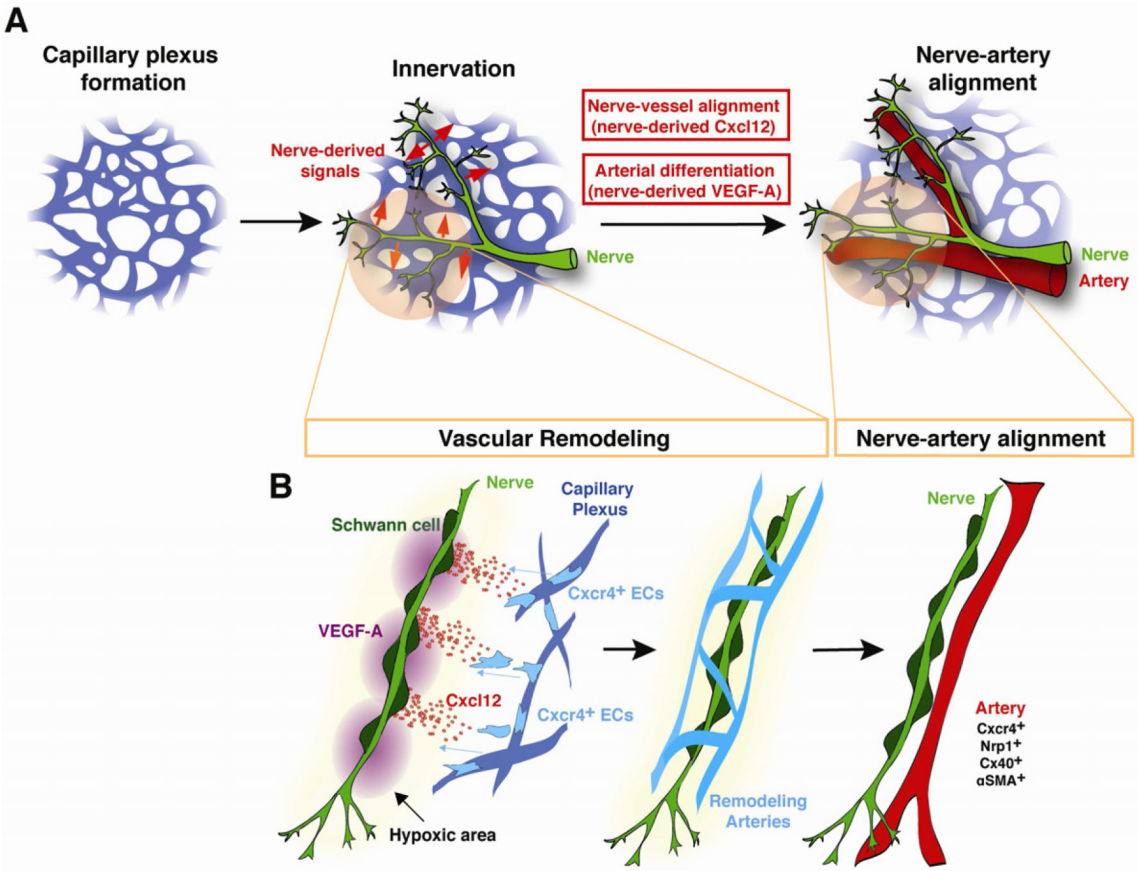

Figure 7. Coordinate action of nerve-derived Cxcl12 and VEGF-A results in nerve-artery alignment

(A) Schematic model for nerve-mediated vascular branching and arterial differentiation in developing limb skin. Sensory nerves invade at approximately E11.5~13.5, after a primary capillary plexus is established. Subsequently, the pattern of sensory nerves provides signals (Cxcl12 and VEGF-A) that govern patterns of vascular branching and arterial differentiation during vascular remodeling. As a result, the congruence of blood vessel and nerve patterns is established in the skin. (B) This scheme shows how nerve-derived Cxcl12 and VEGF-A control patterns of vascular branching and arterial differentiation. In this view, oxygen-starved nerves may induce Cxcl12 and VEGF-A expression through activation of HIF-1 prior to vascular remodeling. Cxcl12-Cxcr4 signaling functions as a long-range chemotactic guidance cue to recruit vessels to align with nerves. Nerve-derived VEGF-A instructs arterial differentiation in the nerve-associated vessels. Arterial differentiation presumably requires a local-action of VEGF-A to induce arterial marker expression.